Ain Shams Engineering Journal 15 (2024) 102419

Contents lists available at ScienceDirect

Ain Shams Engineering Journal

journal homepage: www.sciencedirect.com

Heat transfer analysis of unsteady MHD slip flow of ternary hybrid Casson fluid through nonlinear stretching disk embedded in a porous medium

Dolat khan [a,b], Gohar Ali [d], Poom Kumam [a,b,c,*], Kanokwan Sitthithakerngkiet [e], Fahd Jarad [f]

[a] Fixed Point Research Laboratory, Fixed Point Theory and Applications Research Group, Center of Excellence in Theoretical and Computational Science (TaCS-CoE), Faculty of Science, King Mongkut's University of Technology Thonburi (KMUTT), 126 Pracha Uthit Rd., Bang Mod, Thung Khru, Bangkok 10140, Thailand
[b] Center of Excellence in Theoretical and Computational Science (TaCS-CoE), Faculty of Science, King Mongkut's University of Technology Thonburi (KMUTT), 126 Pracha Uthit Rd., Bang Mod, Thung Khru, Bangkok 10140, Thailand
[c] Department of Medical Research, China Medical University Hospital, China Medical University, Taichung 40402, Taiwan
[d] Department of Mathematics, City University of Science & Information Technology, Peshawar, KPK, Pakistan
[e] Intelligent and Nonlinear Dynamic Innovations Research Center, Department of Mathematics, Faculty of Applied Science, King Mongkut's University of Technology North Bangkok (KMUTNB), 1518, Wongsawang, Bangsue, Bangkok 10800, Thailand
[f] Department of Mathematics, Cankaya University, Etimesgut, Ankara, Turkey

ARTICLE INFO

Keywords:
Casson fluid
Ternary hybrid nanofluid
nonlinear stretching Disk
Porous Medium
Heat transfer analysis

ABSTRACT

The original article's purpose is to assess transfer of heat exploration for unsteady magneto hydrodynamic slip flow of ternary hybrid Casson fluid via a nonlinear flexible disk placed within a perforated medium of a magnetic field in the presence. Unsteady nonlinearly stretched disk inside porous material causes flow to occur. In the investigation, convective circumstances on wall temperature are also considered. The governing equations (PDEs) are transformed into ordinary differential equations (ODEs) using appropriate transformations, and the Keller-box technique is employed for their solution. In forced convection, the variable radiation has no direct impact on fluid velocity, but it is noticed that in the case of aiding flow, fluid velocity rises with an increase in radiation parameter, and the opposite is true in the case of opposing flow. Furthermore, it is experiential that fluid concentration and velocity goes up in creative chemical reactions, and both profiles decrease in detrimental chemical reactions. Moreover, a slightly greater unsteadiness characteristic lowers fluid, concentration, temperature and velocity. Physical parameters' effects on fluid temperature, concentration, and velocity, as well as on wall shear stress, energy, and mass transfer rates, are studied.

1. Introduction

Normal heat transfer fluids cannot be used to meet cooling rate requirements. Such fluids are weaker thermal conductivities are the cause of this. The heat conductivity of ethylene glycol, water, and motor oil is poor. Due to high range of nanofluids they are used in mechanical engineering, industrial engineering and biomedical engineering. Cancer therapy, Cooling of electronic devices, and water distillation are due to nanofluids. Magneto nanofluids are used in magneto hydrodynamics, cancer therapy, cancer tumor treatment, power generators, and many others. The materials known as nanofluids are those that contain trace amounts of 1–100 nm-sized nanoparticles, also referred to as nanoparticles. The carbides, metals, and oxides, such as copper and gold, as well as oxides such as Titania, alumina and copper oxide, make up the nanoparticles. Nanofluids have also been used with diamond and carbon nanotubes. These particles can enhance the base liquids' thermo physical properties. Moreover, magnetic nanofluids are a solid structure with both liquid and magnetic properties. When dealing with conditions like cooling nuclear reactors with liquid sodium, magnetic field interaction with nanofluids is beneficial. Firstly Choi [1], investigated the thermal properties of nanoparticles. Buongiorno [2] researched a model for base fluid thermal properties. A model of a nanomaterial's stagnation point flow toward an extended piece was computed by Mustafa et al. [3]. Turkyilmazoglu [4] discovers the precise solution for magneto hydro dynamics slip flow energy and mass transfer. A model for convective boundary-layer flow of nanoparticles examined by Nield et al. [5]. While Shamshuddin et al. [6] simulate the Von Karman whirling bioconvection

* Corresponding author at: Fixed Point Research Laboratory, Fixed Point Theory and Applications Research Group, Center of Excellence in Theoretical and Computational Science (TaCS-CoE), Faculty of Science, King Mongkut's University of Technology Thonburi (KMUTT), 126 Pracha Uthit Rd., Bang Mod, Thung Khru, Bangkok 10140, Thailand.
E-mail address: poom.kum@kmutt.ac.th (P. Kumam).

https://doi.org/10.1016/j.asej.2023.102419
Received 12 December 2022; Received in revised form 3 July 2023; Accepted 22 July 2023
Available online 8 August 2023

Nomenclature

u, v, w:	velocity components
β:	Casson fluid parameter
ν_{nf}:	nanofluid kinematic viscosity
ρ_{nf}:	nanofluid density
k_{nf}:	nanofluid thermal conductivity
B_0:	magnetic field strength
T_w:	wall temperature
k^*:	mean absorption coefficient
Pr:	Prandtl number
Bi:	Biot number
M:	Magnetic field parameter
(r, z):	Cartesian coordinates
P:	pressure
μ_{nf}:	nanofluid dynamic viscosity
α_{nf}:	nanofluid thermal diffusivity
$(C_p)_{nf}$:	nanofluid specific heat transfer
T_∞:	ambient temperature
σ^*:	Stefan-Boltzmann constant
k_0:	porosity parameter
Ec:	Eckert number
K:	Porous medium
δ:	slip parameter

Table 1
The base liquid's and nanomaterial's thermophysical properties.

Material	Base fluids			
	SA	Al_2O_3	*Cu*	*Ag*
$\rho(\mathrm{kg/m^3})$	989	3970	8933	10,500
$K(\mathrm{W/m\,K})$	0.613	40	401	429
$c_p(\mathrm{J/kg\,K})$	4175	765	385	235
$\beta \times 10^{-5}(\mathrm{K}^{-1})$	0.99	0.85	1.67	1.89
Pr	6	–	–	–

nanofluid flow using the Adomian decomposition technique. [7,8]. Furthermore, in [9–11] the effect of radiative heat on nanofluid flows. They address a variety of topics, including nanofluid flow in a parallel channel with thermal buoyancy, stability analysis of a stretching/shrinking sheet, and axisymmetric nanofluid flow with reactions in porous media. These research provide light on convective heat transfer augmentation, dual solutions, and the behavior of nanofluids in complicated flow settings, all of which have practical relevance. Animasaun et al. [12] explores the thermal analysis of unsteady water-based ternary hybrid nanofluids on wedges, considering bioconvection, wall stretching velocity, and different magnitudes of nanoparticle thermal conductivity. The dynamics of ternary-hybrid nanofluids on wedge surfaces under forced convection are examined in the paper by Xiu et al. [13] which takes into account variable water temperatures as well as small and large quantities of nanoparticles. (Table 1).

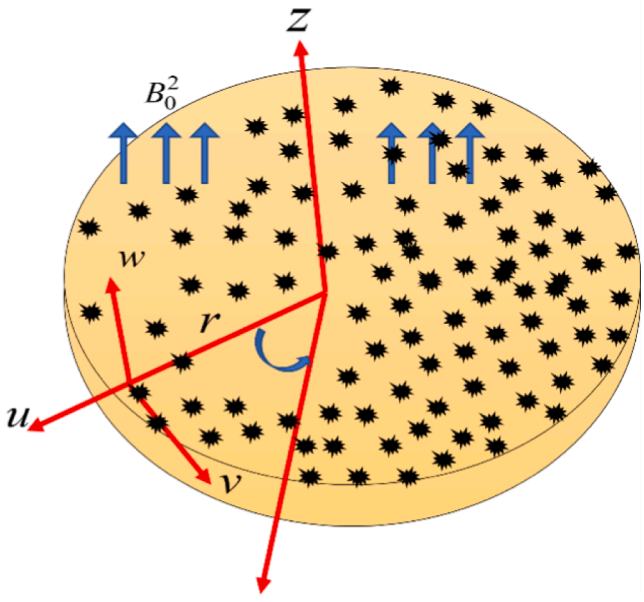

Fig. 1. Geometrical configuration of the model.

Hybrid nanofluids are classified as combinations or mixtures of two nanomaterials that are uniformly dispersed within a base liquid. When compared to nanofluids, hybrid nanofluids is more productive both monetarily and thermal. This new category of liquids denotes a liquid combination that has nano particles of two different solids distributed throughout one liquid. Hybrid nanoparticles have different thermal conductivity from base liquid. This kind of liquid has more uses related to the heating process and performs well in cooling where the temperature range is high. Hybrid nanofluids have numerous uses in the fields of refrigeration, solar energy, and industrial. Kshirsagar and Venkatesh [14] analysis of the setup of several apparatuses and investigation of the factors affecting hybrid nano-fluid performance. According to their conclusions, hybrid nanomaterials have higher heat conductivity than nanoparticles. A technique for calculating the conductivity of thermal of this fluids containing nanomaterials was scrutinized by Chen et al. [15]. The stability for dual solutions is examined in a simulation of time-dependent radiative heat transport across a stretching/shrinking sheet of hybrid nanofluid by Tinker et al. [10]. The MHD flow of a viscous fluid across a flat plate under a low-pressure gradient is examined using the Homotopy Perturbation Method by Pattnaik, and Mishra [16]. In a computational research utilising a non-Fourier heat flux model, Shamshuddin et al. [17] examine heat transfer and viscous flow in a dual rotating extensible disc system. A numerical investigation on the impact of chemical reaction on magnetohydrodynamic flow across an exponential stretching sheet is done by Pattnaik et al. [18]. Due to the widespread usage of hybrid nanofluids, researchers have created a number of models for hybrid nanomaterials and have determined that they have a far higher thermal conductivity than nanofluids [19,20].

Casson fluid, a very effective non-Newtonian fluid, is used to assess inks, emulsions, food items, certain viscoelastic materials, and water colours. This fluid is one of the finest ones used today to mimic shear thinning liquids with rod-like components. In contrast to other fluid models like the power law, the Casson fluid model is capable of accepting complex rheological representative of a fluid. Cassion and Dash compute the fluid flow properties of a Casson fluid in a cylinder filled with a uniform porous medium [21,22]. Pham et al [23] mathematical study of the Cassion fluid led to the discovery of exit flows characterized by sudden contraction and a yield stress. Using velocity and temperature slip consequences, Amanullah et al. [24] investigated at the two-dimensional, laminar, energy and mass transfer of spontaneously convective micro liquid flow across a semi-infinite vertical plate surface. In a study to examine the effects of fluid viscosity, variable

thermal conductivity, and nonlinear radiation on magnetohydrodynamic Casson nanofluid flow over a flat plate, Ghadikolaei et al. [25] found that velocity increases with an increase in variable thermal conductivity and viscosity while temperature and the volume fraction of nanoparticles decreases at a certain temperature. Das et al. [26] looked into the unsteady magnetohydrodynamics of chemically reactive double-diffusive Casson fluid on a level surface with heat and mass transfer. Mobile microorganisms can be beneficial for the suspension of nanofluids since they aid to preserve the distributed nanoparticles. It is important to note that the aforementioned study did not account for the lack of moving microorganisms.

On the basis of comprehensive literature review this article's goal aimed to evaluate heat transfer research into the porous medium of a magnetic field and the unsteady magneto hydrodynamic slip flow of a ternary hybrid Casson fluid through a nonlinear flexible disk. Flow is brought about by an unstable, nonlinearly stretched disk deep inside the porous material. Convective conditions on wall temperature are also taken into account in the study.

2. Mathematical formulation

We investigate a viscoelastic radiative fluid flow of a Casson trihybrid nanofluid, which consists of a mixture of nanoparticles, around a rotating disc. In this study, we consider the presence of three different types of nanoparticles within a single fluid. Additionally, we account for the influence of non-linear thermal radiation. The rotating disc is assumed to be in the xy-plane at $z = 0$, as shown in Figure 1. Our primary focus is to analyze the impact of the newly developed nanofluid model, known as "trihybrid nanofluid," on the fluid flow over the rotating disc. The continuity equation for the mixed convective flow of the Casson fluid is as follows:

$$\frac{\partial u}{\partial r}+\frac{\partial w}{\partial z}+\frac{u}{r}=0 \tag{1}$$

$$\frac{\partial u}{\partial t}+\frac{u\,\partial u}{\partial r}+\frac{w\,\partial u}{\partial z}-\frac{v^2}{r}=-\frac{\partial p}{\partial r}\frac{1}{\rho_{nf}}+\nu_{nf}\left(r^{-1}\frac{\partial u}{\partial r}+\frac{\partial^2 u}{\partial r^2}+\frac{\partial^2 u}{\partial z^2}-\frac{u}{r^2}\right)-\frac{B_0^2\sigma_{nf}u}{\rho_{nf}} \tag{2}$$

$$\frac{\partial v}{\partial t}+\frac{u\,\partial v}{\partial r}+\frac{w\,\partial v}{\partial z}+\frac{uv}{r}=\nu_{nf}\left(\frac{\partial}{\partial r}\left(v\frac{1}{r}\right)+\frac{\partial^2 v}{\partial r^2}+\frac{\partial^2 v}{\partial z^2}\right)-\frac{B_0^2\sigma_{nf}v}{\rho_{nf}}-\frac{\nu_{nf}}{k_0}v \tag{3}$$

$$\frac{\partial w}{\partial t}+\frac{w\partial w}{\partial z}+\frac{u\partial w}{\partial r}+\;=\;-\frac{\partial p}{\partial r}\frac{1}{\rho_{nf}}+\nu_{nf}\left(r^{-1}\frac{\partial w}{\partial r}+\frac{\partial^2 w}{\partial r^2}+\frac{\partial^2 w}{\partial z^2}\right) \tag{4}$$

$$\frac{\partial T}{\partial t}+w\frac{\partial T}{\partial z}+u\frac{\partial T}{\partial r}=\alpha_{nf}\left(\frac{\partial^2 T}{\partial r^2}+\frac{\partial^2 T}{\partial z^2}+\frac{1}{r}\frac{\partial T}{\partial r}\right)-\frac{1}{(\rho C_p)_{nf}}\partial q_r\frac{1}{\partial z} \tag{5}$$

By using the following BCs:

$$\left.\begin{array}{c} v=\Omega r,\;\; u=\xi r\,,\;\; w=0,\\ T\to T_w,\;\; at\;\; z=0\\ v\to 0,\;\; u\to 0\,,\\ T\to T_\infty\;\; as\;\; z\to\infty, \end{array}\right\} \tag{6}$$

Here P for pressure, $\nu_{nf}=\frac{\mu_{nf}}{\rho_{nf}}$ kinematic viscosity and $\alpha_{nf}=\frac{k_{nf}}{(\rho C_p)_{nf}}$ represent thermal diffusivity.

The Rosseland diffusion approximation for radiation is:

$$q_r=\frac{-4\sigma^*}{3k^*}\frac{\partial T^4}{\partial z} \tag{7}$$

Stefan-Boltzmann constant is represent by σ^*. k^* for mean absorption coefficient. T_4 for temperature linear function. To expand T^4 using Taylor series with T^1 and remove higher terms, we can describe

$$T^4\;\cong\;-3T_\infty^4+4T_\infty^3\,T \tag{8}$$

Put Equation (9) and Equation (10) in Equation (4), as we get:

$$\frac{\partial T}{\partial t}+\frac{u\partial T}{\partial r}+\frac{w\partial T}{\partial z}=\alpha_{nf}\left(\frac{\partial^2 T}{\partial r^2}+r^{-1}\frac{\partial T}{\partial r}+\frac{\partial^2 T}{\partial z^2}\right)-\left(\frac{16\sigma^* T_\infty^3}{3k_1^*(\rho C_p)_{nf}}\right)\frac{\partial^2 T}{\partial z^2} \tag{9}$$

$$\frac{\partial T}{\partial t}+\frac{u\partial T}{\partial r}+\frac{v\partial T}{\partial z}=\frac{k_{thnf}}{(\rho c_p)_{thnf}}\left(\frac{\partial^2 T}{\partial r^2}+r^{-1}\frac{\partial T}{\partial r}+\frac{\partial^2 T}{\partial z^2}\right)-\frac{1}{(\rho c_p)_{thnf}}\frac{16\sigma^* T_\infty^3}{3k_1^*}\frac{\partial^2 T}{\partial z^2}$$
$$+\frac{\nu_{thnf}}{(c_p)_{thnf}}\left(1+\frac{1}{\beta}\right)\left(\left(\frac{\partial u}{\partial z}\right)^2+\left(\frac{\partial v}{\partial z}\right)^2\right)+\frac{\sigma_{thnf}B_0^2}{(\rho c_p)_{thnf}}(u^2+v^2)+\frac{Q(T-T_\infty)}{(\rho c_p)_{thnf}}, \tag{10}$$

by also provide the stream function (ψ), described in terms of velocity in its standard notation, with a variable (η), and the transformations shown below;

$$\eta=\sqrt{\frac{(n+1)\nu}{2\nu(1-\gamma t)}}r^{\frac{n-1}{2}}z,\;\psi=\sqrt{\frac{2c\nu}{(n+1)(1-\gamma t)}}r^{\frac{n+1}{2}}f(\eta),\vartheta=\frac{T-T_\infty}{T_f-T_\infty} \tag{11}$$

By using Eq. (8), the system of Eqs. (1–3) and (7)

$$A\left(\frac{\eta f^{'''}}{n+1}+\frac{2f^{'}}{n+1}\right)=\left(1+\frac{1}{\beta}\right)f^{'''}+ff^{''}-\frac{2nf^{'2}}{n+1}-(K+M)f^{'}+\lambda\,\vartheta \tag{12}$$

$$\left(1+\frac{4}{3}R_d\right)\vartheta^{''}+Prf\vartheta^{'}-\frac{2(2n-1)}{n+1}Prf^{'}\vartheta+Pr\left(1+\frac{1}{\beta}\right)Ecf^{''2}+PrMEcf^{'2}$$
$$+Pr\varepsilon\vartheta=PrA\left(\frac{2(2n-1)}{n+1}\vartheta+\frac{1}{n+1}\eta\vartheta^{'}\right) \tag{13}$$

$$\begin{aligned} &f^{'}(0)=1+\left(1+\frac{1}{\beta}\right)\delta f^{''}(0),\\ &\vartheta^{'}(0)=-(1-\vartheta(0))Bi\\ &\vartheta(\infty)=0\,,\;\; f^{'}(\infty)=0 \end{aligned} \tag{14}$$

Where

$$M=\frac{2\sigma_f B_0^2}{\rho_f c(n+1)},\;K=\frac{2\nu_f\varphi}{k_0(n+1)c},\;\;\lambda=N_0\sqrt{\frac{(n+1)c}{2\nu_f}},\;Bi=\frac{h_0}{k_f}\left\{\frac{2\nu_f}{c(n+1)}\right\}^{\frac{1}{2}},$$

$$R_d=\frac{4\sigma^* T_\infty^3}{\alpha k_1^*},Pr=\frac{\mu_f(c_p)_f}{k_f},\;\;Ec=\frac{u_w^2}{(c_p)_f(T_f-T_\infty)},\;\varepsilon=\frac{Q_0}{(\rho c_p)_f(n+1)c},$$

$$\delta=N_0\sqrt{\frac{(n+1)c}{2\nu_f}},$$

$$\mu_{thnf}=\frac{\mu_f}{(1-\phi_{s2})^{2.5}(1-\phi_{s1})^{2.5}(1-\phi_{s3})^{2.5}}$$

$$\rho_{thnf}=\rho_f(1-\phi_{s2}-\phi_{s1}-\phi_{s3})+\rho_{s1}\phi_{s1}+\rho_{s3}\phi_{s3}+\rho_{s2}\phi_{s2}\qquad (\rho\beta_T)_{thnf}=(1-\phi_{s1}-\phi_{s2}-\phi_{s3})(\rho\beta_T)_{bf}+(\rho\beta_T)_{s2}\phi_{s2}+(\rho\beta_T)_{s3}\phi_{s3}+(\rho\beta_T)_{s1}\phi_{s1}$$
$$(\rho C_p)_{thnf}=(\rho C_p)_{bf}(1-\phi_{s3}-\phi_{s1}-\phi_{s2})+\phi_{s2}(\rho C_p)_{s2}+\phi_{s3}(\rho C_p)_{s3}+\phi_{s1}(\rho C_p)_{s1}$$

$$\frac{K_{nf}}{K_f}=\left\{\frac{K_{s3}+2K_f-2\phi_{s3}(K_f-K_{s3})}{K_{s3}+2K_f+\phi_{s3}(K_f-K_{s3})}\right\},\frac{K_{hnf}}{K_{nf}}=\left\{\frac{K_{s2}+2K_{nf}-2\phi_{s1}(K_{nf}-K_{s1})}{K_{s1}+2K_{nf}+\phi_{s1}(K_{nf}-K_{s1})}\right\},$$
$$\frac{K_{thnf}}{K_{hnf}}=\left\{\frac{K_{s2}+2K_{hnf}-2\phi_{s2}(K_{hnf}-K_{s2})}{K_{s2}+2K_{hnf}+\phi_{s2}(K_{hnf}-K_{s2})}\right\}.$$

$$\sigma_{nf}=\sigma_f\left\{\frac{\sigma_{s3}(1+2\phi_{s3})+\sigma_f(1-2\phi_{s3})}{\sigma_{s3}(1-\phi_{s3})+\sigma_f(1+\phi_{s3})}\right\},\sigma_{hnf}=\sigma_{bf}\left\{\frac{\sigma_{s2}(1+2\phi_{s2})+\sigma_{nf}(1-2\phi_{s2})}{\sigma_{s2}(1-\phi_{s2})+\sigma_{nf}(1+\phi_{s2})}\right\},$$
$$\sigma_{thnf}=\sigma_{hnf}\left\{\frac{\sigma_{s1}(1+2\phi_{s1})+2\sigma_{hnf}(1-2\phi_{s1})}{\sigma_{s1}(1-\phi_{s1})+\sigma_{hnf}(2+\phi_{s1})}\right\}$$

$$g_1=\frac{1}{(1-\phi_{s1})^{2.5}(1-\phi_{s2})^{2.5}(1-\phi_{s3})^{2.5}}$$

$$g_2=1-\phi_{s2}-\phi_{s1}-\phi_{s3}+\phi_{s1}\frac{\rho_{s1}}{\rho_f}+\phi_{s3}\frac{\rho_{s3}}{\rho_f}+\phi_{s2}\frac{\rho_{s2}}{\rho_f}$$
$$g_3=1-\phi_{s1}+\phi_{s1}\frac{(\rho\beta_T)_{s1}}{(\rho\beta_T)_f}-\phi_{s2}-\phi_{s3}+\phi_{s2}\frac{(\rho\beta_T)_{s2}}{(\rho\beta_T)_f}+\phi_{s3}\frac{(\rho\beta_T)_{s3}}{(\rho\beta_T)_f}$$
$$g_4=1-\phi_{s1}-\phi_{s2}+\phi_{s1}\frac{(\rho C_p)_{s1}}{(\rho C_p)_{bf}}-\phi_{s3}+\phi_{s2}\frac{(\rho C_p)_{s2}}{(\rho C_p)_{bf}}+\phi_{s3}\frac{(\rho C_p)_{s3}}{(\rho C_p)_{bf}}$$

$$g_5=\frac{K_{thnf}}{K_f}g_6=\frac{\sigma_{thnf}}{\sigma_f}$$

$$\frac{\partial u}{\partial t}+u\frac{\partial u}{\partial x}+v\frac{\partial v}{\partial y}=\frac{g_1}{g_2}\left(1+\frac{1}{\beta}\right)\frac{\partial^2 u}{\partial y^2}-\left(\frac{g_6}{g_2}\frac{\sigma_{thnf}B_0^2}{\rho_{thnf}}+\frac{g_1}{g_2}\frac{\nu_{thnf}\varphi}{k_1}\right)u+\frac{g_3}{g_2}g(\beta_T)_{thnf}(T-T_\infty) \quad (15)$$

$$\frac{g_1}{g_2}\left(1+\frac{1}{\beta}\right)f'''+ff''-\frac{2n}{n+1}f'^2-\left(\frac{g_6}{g_2}M+\frac{g_1}{g_2}K\right)f'+\lambda\frac{g_3}{g_2}\vartheta=A\left(\frac{2}{n+1}f'+\frac{1}{n+1}\eta f''\right) \quad (16)$$

$$\frac{g_5}{g_4}\left(1+\frac{4}{3}R_d\right)\vartheta''+Prf\vartheta'-\frac{2(2n-1)}{n+1}Prf'\vartheta+\frac{g_1}{g_4}Pr\left(1+\frac{1}{\beta}\right)Ecf''^2+\frac{g_6}{g_4}PrMEcf'^2+\frac{1}{g_4}Pr\varepsilon\vartheta=PrA\left(\frac{2(2n-1)}{n+1}\vartheta+\frac{1}{n+1}\eta\vartheta'\right) \quad (17)$$

3. Results and discussion

Through the use of a nonlinear stretch disk embedded in a porous medium, this work aims to enhance heat transfer analysis of unsteady magneto hydrodynamic slip flow of ternary hybrid Casson fluid. To

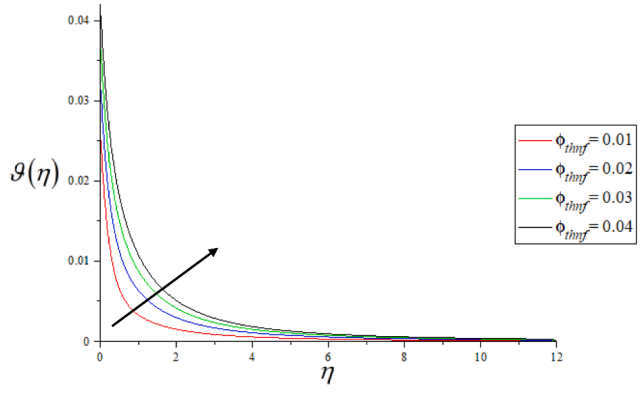

Fig. 2. Consequence of ϕ_{thnf} on Temperature of fluid.

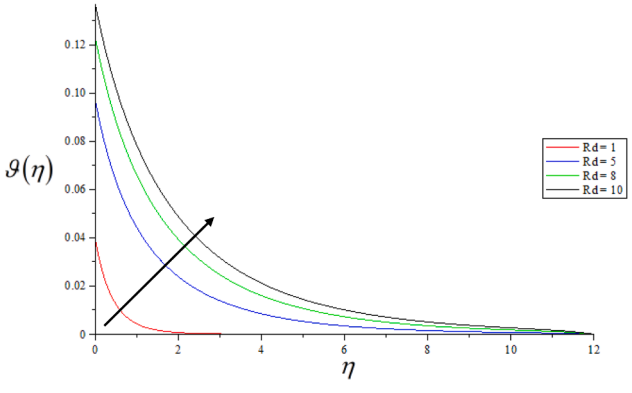

Fig. 3. Consequence of *Rd* on temperature of fluid.

resolve the problem, we used a Matlab program and the Keller-box strategies as the details are in the following flow chart.

Flow chart.

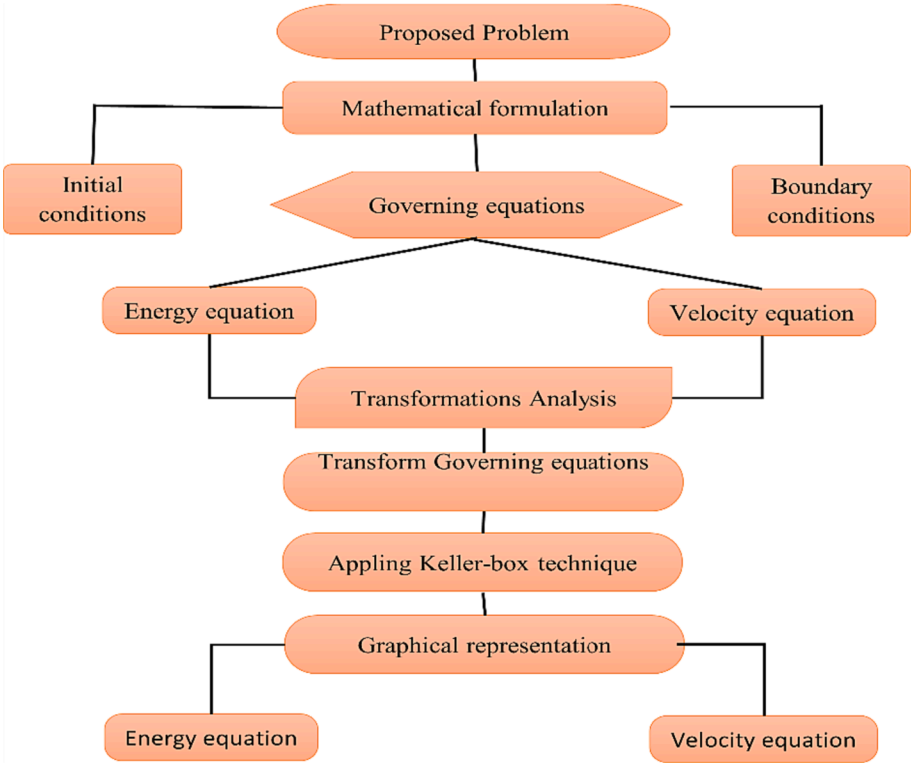

4. Temperature profile

The influences of several parameters are plotted for temperature profile in figures 2-11 and velocity profile in figures 12-21.

The volume fraction effect of tri-hybrid nanofluids is presents in figure 2 and figure 12 for temperature and velocity respectively. The enhancement of volume fractional enhance the temperature profile while decrease the velocity of the fluid. This result is due to the tri nanofluid being added to the base liquid, which strengthens the viscous forces in the trihybrid nanofluid.

Figure 3 and figure 13 are plotted to displays the consequence of *Rd* on temperature and velocity profiles. The greater value of radiation parameter enhances the temperature profile and fluid velocity. Physically, this is true because larger values of *Rd* result in a greater radiation impact, which increases the thermal boundary layer thickness as a result both profiles are enhance.

Figure 4 and figure 14 demonstrate the effect of *n* on both velocity and temperature profiles. The thickness of the thermal and velocity boundary layers are both rapidly reduced as the parameter *n* is increased.

A declining tendency in the velocity profile has been seen as a result of the Lorentz force, which is generated as *M* increases and slows the fluid's motion. The temperature profile of the fluid is also impacted by the Lorentz force. The thermal boundary layer thickens because electromagnetic forces are stronger than viscous forces at larger values of *M*. Figure 15 and Figure 5 show these outcomes, respectively.

The effects of *K* on the temperature and velocity profiles were highlighted in Figures 6 and 16, respectively. Physically, the size of the

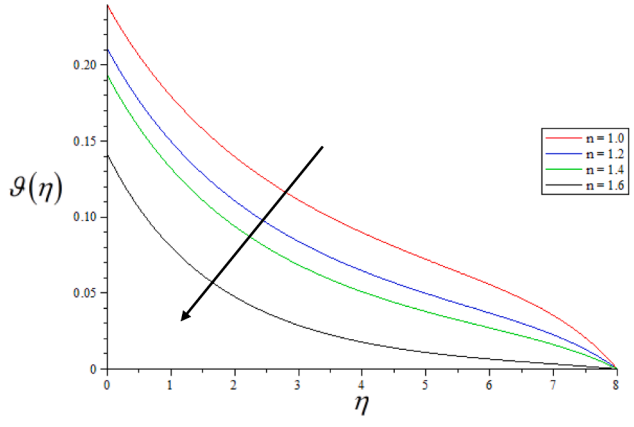

Fig. 4. Consequence of *n* on Temperature of fluid.

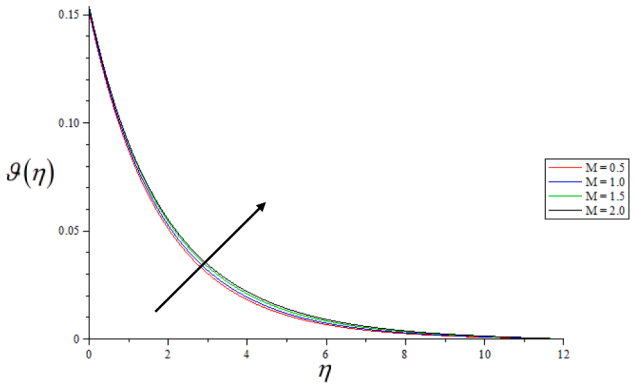

Fig. 5. Consequence of *M* on Temperature of fluid.

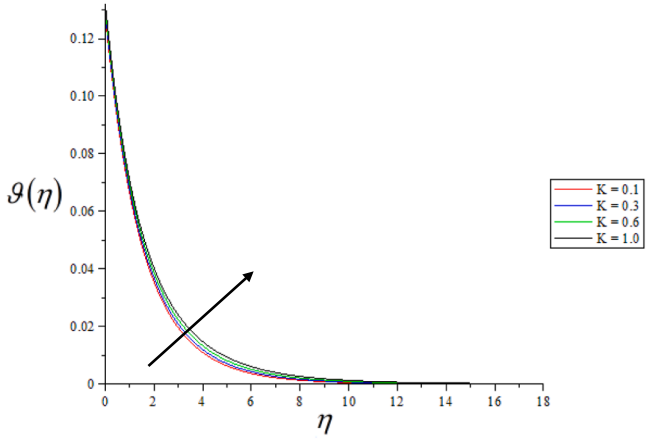

Fig. 6. Consequence of K on Temperature of fluid.

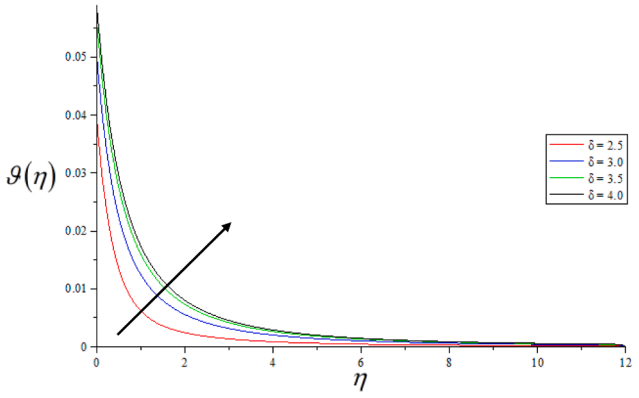

Fig. 7. Consequence of δ on Temperature of fluid.

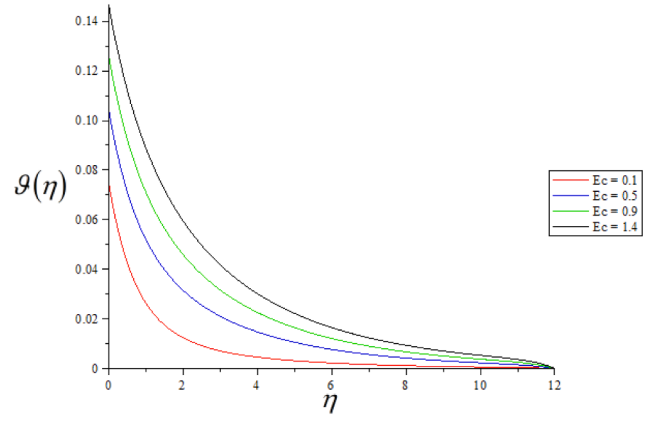

Fig. 8. Consequence of Ec on Temperature of fluid.

pores in porous media widens as K rises; in this scenario, the drag force acting against the flow direction causes the velocity boundary layer thickness to decrease and the velocity to be retarded. In contrast to unsteady flow, stable flow exhibits a stronger impact of K and a thicker thermal boundary layer.

Figure 7 and figure 17 shows the outcomes of δ on temperature and velocity profiles. It observed that the slipping parameter enhance the temperature of the fluid while the rapidly decrease the fluid velocity. This behavior can be explained by the fact that as flow near the disk decreases and more fluid is allowed to slip over the disk, the slip effect toward the free stream becomes less strong.

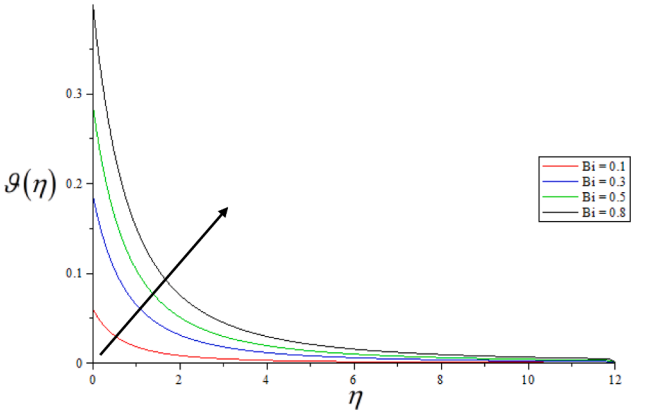

Fig. 9. Consequence of Bi on Temperature of fluid.

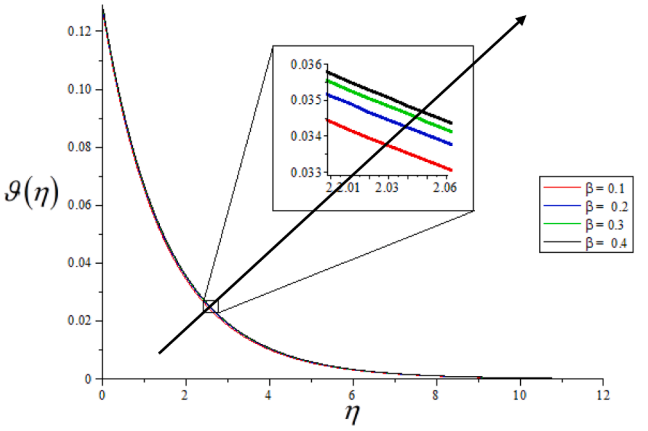

Fig. 10. Consequence of β on Temperature of fluid.

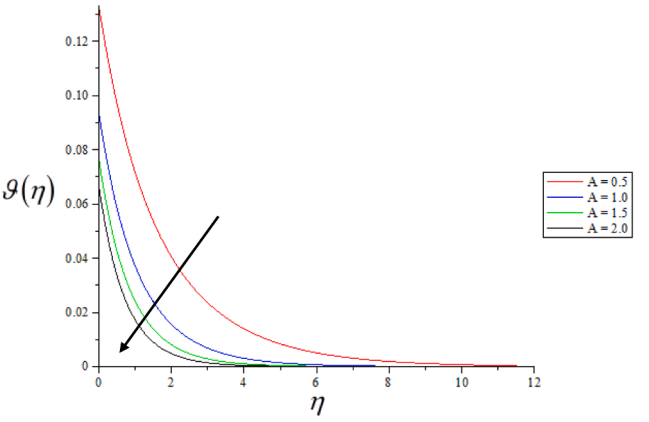

Fig. 11. Consequence of A on Temperature of fluid.

Figures 8 and 18 show how the Eckert number Ec responds to heat transfer and fluid velocity. As the amplitude of rises Ec, a rinsing tendency is visible in both profiles. Since it represents the proportion of the boundary layer's kinetic energy to its enthalpy difference, this is a physically sound statement. Since a positive signifies that heat has been transferred from the plate to the fluid, the temperature of the fluid rises as viscous heat dissipation increases.

Consequences of fluid temperature and velocity profile are shown in Figures 9 and 19. The ratio of the thermal resistance inside the disk to that of the boundary layer of the hot fluid at the surface's bottom is known as the Biot number. Temperature is an increasing function of Bi in

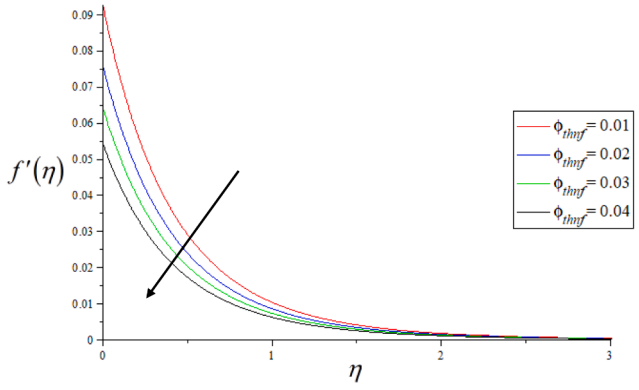

Fig. 12. Consequence of ϕ_{thnf} on velocity of fluid.

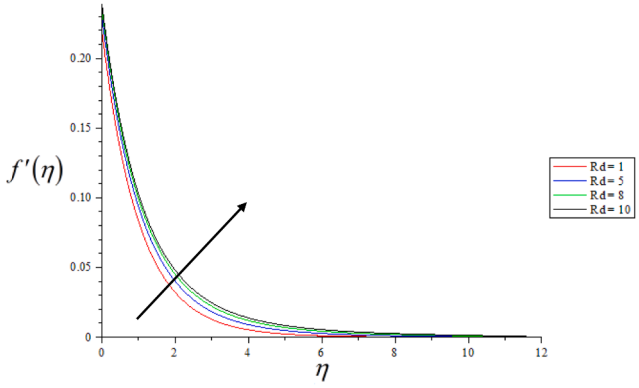

Fig. 13. Consequence of *Rd* on velocity of fluid.

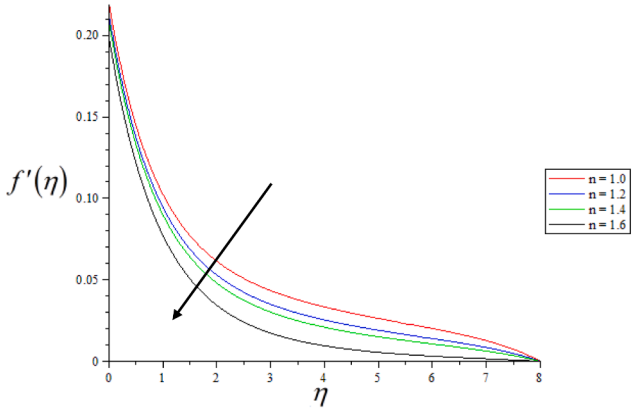

Fig. 14. Consequence of *n* on Velocity of fluid.

each of these scenarios. Convection at the surface is strengthened by the force, which causes a rise in surface temperature and, as a result, an increase in fluid velocity.

Clearly, Figure 10 and figure 20 depicts that the greater value of β caused the enhancement of heat transfer profile and fluid velocity close to the plate while fall the velocity gone from the plate. This occurrence demonstrates how a drop in yield stress can result in an rise in the thickness of the thermal boundary layer. Furthermore, the impact is exacerbated for linearly expanding disks that are not completely stable.

Lastly, figures 11 and 21 show the analysis of *A* on both temperature and velocity profiles. Both velocity and temperature fluid are

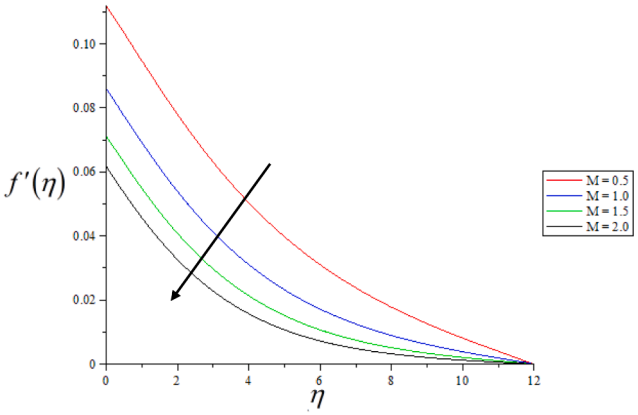

Fig. 15. Consequence r of *M* on Velocity of fluid.

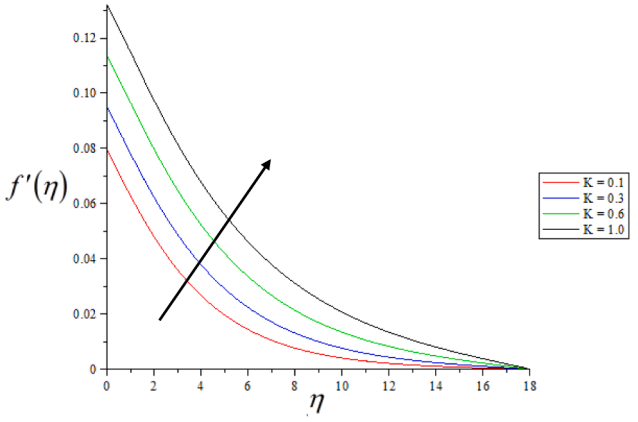

Fig. 16. Consequence of *K* on Velocity of fluid.

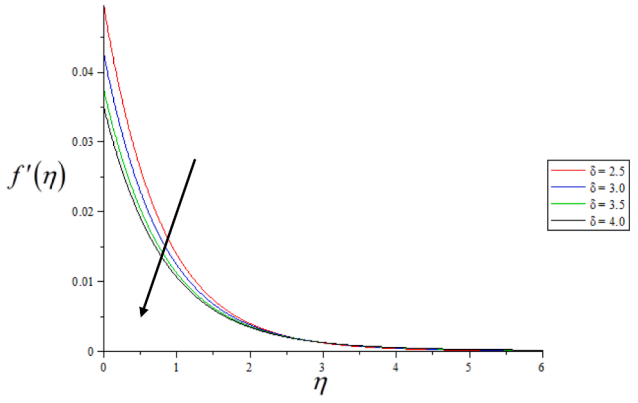

Fig. 17. Consequence of δ on Velocity of fluid.

appreciated to fall as *A* enhances. We also see that the boundary layer is thinner for greater *A* amplitudes.

The assessment of skin frictional of the present papers is compared with Nadeem et al. [27], Oyelakin et al. [28] and Ullah et al. [29] in Table 2, which shows a good agreement to existing literature. Table 3 present the comparison of heat transfer rate of the tri hybrid nanofluid to the classical and hybrid nanofluid, it is observed that the ternary hybrid nanofluid enhance the rate of heat transfer up-to 38.88529% as compared to the classical fluid.

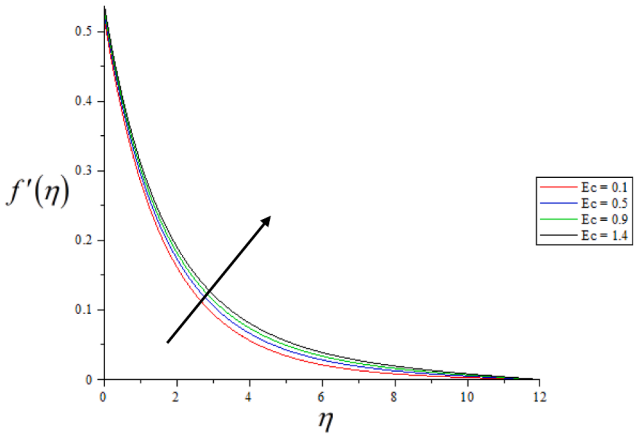

Fig. 18. Consequence of *Ec* on Velocity of fluid.

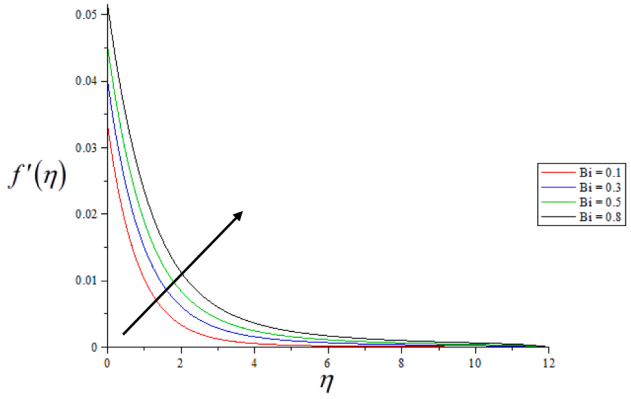

Fig. 19. Consequence of *Bi* on Velocity of fluid.

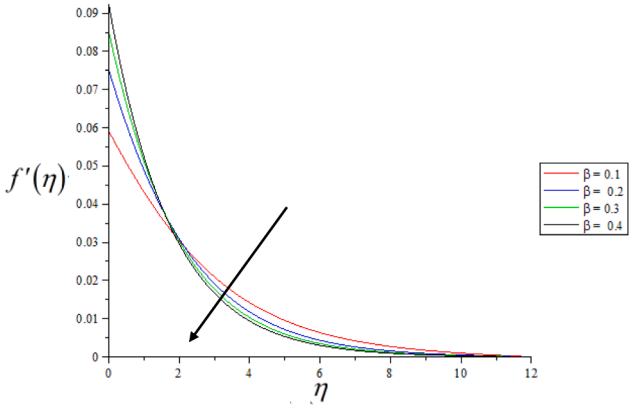

Fig. 20. Consequence of β on Velocity of fluid.

5. Conclusion

With convective conditions on wall temperature taken into consideration, the current work intends to analyse the heat transfer of unsteady magnetohydrodynamics slip flow of ternary hybrid Casson fluid through a nonlinear stretching disk embedded in a porous medium. The Keller-box approach should be used to solve the issue. The core ideas of this book are as follows:

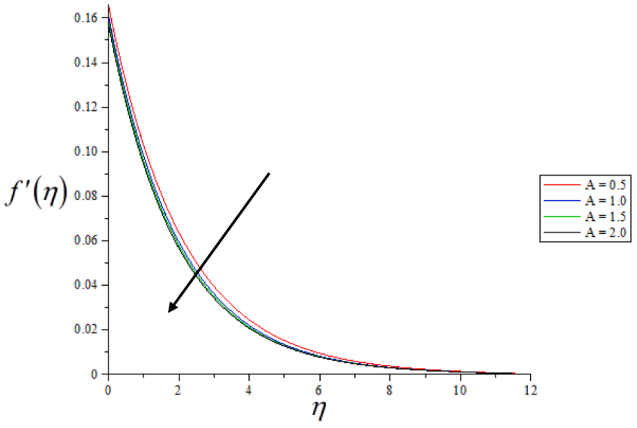

Fig. 21. Consequence of *A* on Velocity of fluid.

Table 2
Skin friction comparison for various values of *M* and β when $Bi \to \infty$, $n = 1, A = M = K = N = R_d = Sc = R = \lambda = \delta = \phi_1 = \phi_2 = 0$.

$f''(0)\left(1+\frac{1}{\beta}\right)$

M	β	Nadeem et al. [27]	Oyelakin et al. [28]	Ullah et al. [29]	Present
0	5	-1.0954	-1.0944	-1.0955	-1.09552
0	1	-1.4142	-1.41421	-1.4144	-1.41441
10	5	-3.6331	-3.63318	-3.6332	-3.63320
10	1	-4.6904	-4.69042	-4.6904	-4.69042
100	5	-11.0091	-11.00909	-11.0091	-11.00912
100	1	-14.2127	-14.21267	-14.2127	-14.21271

Table 3
Nu Comparision of Tri Nano fluid with hybrid nano fluid, nanofluid and Classical fluid.

Name fluid	*Nu*	%age
Classical fluid	1.543	
Nanofluid	1.743	12.96176
Hybrid nanofluid	1.943	25.92353
Tri nanofluid	2.143	38.88529

1. By rising the values of *R*, then the result the velocity and concentration profile show the decreasing behavior.
2. Due to the radiation parameter, fluid velocity increases as the radiation parameter grows for a helping flow and drops as the radiation parameter increases for an opposing flow. The radiation parameter has no impact on fluid velocity in the presence of forced convection.
3. As a result of generative chemical reactions, fluid velocity and concentration rise, whereas destructive chemical reactions cause both characteristics to fall.
4. temperature and concentration are shown in the situation of unsteady flow with the effects of *M* and *K*.
5. Temperature is an increasing function of Bi1 in each of these situations. The reason for this is due to the fact that the asset of *Bi* rises the convective at the surface, which in turn leads to a rise in the temperature of the surface and so on the velocity of the fluid also enhance.

Declaration of Competing Interest

The authors declare that they have no known competing financial interests or personal relationships that could have appeared to influence the work reported in this paper.

Acknowledgements

The first author appreciates the support provided by Petchra Pra Jom Klao Ph.D. Research Scholarship through grant no (95/2563), by King Mongkut's University of Technology Thonburi, Thailand. The authors acknowledge the financial support provided by the Center of Excellence in Theoretical and Computational Science (TaCS-CoE), KMUTT. This research was funded by National Science, Research and Innovation Fund (NSRF), and King Mongkut's University of Technology North Bangkok with Contract no. KMUTNB-FF-66-05.

Funding

Moreover, this research project is supported by Thailand Science Research and Innovation (TSRI) Basic Research Fund: Fiscal year 2022 (FF65).

References

[1] Choi SUS, Eastman Jeffrey A.Enhancing thermal conductivity of fluids with nanoparticles. No. ANL/MSD/CP-84938; CONF-951135-29. Argonne National Lab. (ANL), Argonne, IL (United States); 1995.
[2] Buongiorno Jacopo. Convective transport in nanofluids; 2006. p. 240–50.
[3] Mustafa M, et al. Stagnation-point flow of a nanofluid towards a stretching sheet. Int J Heat Mass Transf 2011;54(25-26):5588–94.
[4] Turkyilmazoglu M. Exact analytical solutions for heat and mass transfer of MHD slip flow in nanofluids. Chem Eng Sci 2012;84:182–7.
[5] Nield DA, Kuznetsov AV. The Cheng-Minkowycz problem for natural convective boundary-layer flow in a porous medium saturated by a nanofluid. Int J Heat Mass Transf 2009;52(25-26):5792–5.
[6] Shamshuddin M, Mishra SR, Beg OA, Kadir A. Adomian decomposition method simulation of Von Karman swirling bioconvection nanofluid flow. J Central South Univ: Sci Technol of Min Metall 2019;26(10):2797–813.
[7] Dawar A, Wakif A, Thumma T, Shah NA. Towards a new MHD non-homogeneous convective nanofluid flow model for simulating a rotating inclined thin layer of sodium alginate-based Iron oxide exposed to incident solar energy. Int Commun Heat Mass Transf 2022;130:105800.
[8] Saleem S, et al. Insight into the motion of water conveying three kinds of nanoparticles shapes on a horizontal surface: significance of thermo-migration and Brownian motion. Surf Interfaces 2022;30:101854.
[9] Pattanaik PC, Mishra SR, Jena S, Pattnaik PK. Impact of radiative and dissipative heat on the Williamson nanofluid flow within a parallel channel due to thermal buoyancy. Proc Inst Mech Eng, Part N: J Nanomater, Nanoeng Nanosyst 2022;236 (1–2):3–18.
[10] Shah NA, Wakif A, El-Zahar ER, Thumma T, Yook SJ. Heat transfers thermodynamic activity of a second-grade ternary nanofluid flow over a vertical plate with Atangana-Baleanu time-fractional integral. Alexandria Eng. J. 2022;61 (12):10045–53.
[11] Pattnaik PK, Mishra SR, Bég OA, Khan UF, Umavathi JC. Axisymmetric radiative titanium dioxide magnetic nanofluid flow on a stretching cylinder with homogeneous/heterogeneous reactions in Darcy-Forchheimer porous media: Intelligent nanocoating simulation. Mater Sci Eng B 2022;277:115589.
[12] Animasaun IL, et al. Unsteady water-based ternary hybrid nanofluids on wedges by bioconvection and wall stretching velocity: thermal analysis and scrutinization of small and larger magnitudes of the thermal conductivity of nanoparticles. Mathematics 2022;10(22):4309.
[13] Xiu Weirong et al. Dynamics of ternary-hybrid nanofluids due to dual stretching on wedge surfaces when volume of nanoparticles is small and large: forced convection of water at different temperatures. Int Commun Heat Mass Transf 2022;137: 106241.
[14] Kshirsagar DP, Venkatesh MA. A review on hybrid nanofluids for engineering applications. Mater Today: Proc 2021;44:744–55.
[15] Chen H, Witharana S, Jin Y, Kim C, Ding Y. Predicting thermal conductivity of liquid suspensions of nanoparticles (nanofluids) based on rheology. Particuology 2009;7(2):151–7.
[16] Pattnaik PK, Pattnaik JR, Mishra SR. Illustration of low-pressure gradient on the MHD flow of viscous fluid over a flat plate: the Homotopy Perturbation Method. Waves in Random Complex Media 2022:1–19.
[17] Shamshuddin MD, et al. Numerical study of heat transfer and viscous flow in a dual rotating extendable disk system with a non-Fourier heat flux model. Heat Transf—Asian Res 2019;48(1):435–59.
[18] Pattnaik PK, et al. Influence of chemical reaction on magnetohydrodynamic flow over an exponential stretching sheet: a numerical study. Int J Fluid Mech Res 2020; 47:3.
[19] Krishna VM, et al. Numerical study of fluid flow and heat transfer for flow of Cu-Al2O3-water hybrid nanofluid in a microchannel heat sink. Mater Today: Proc 2022;49:1298–302.
[20] Casson N. Flow equation for pigment-oil suspensions of the printing ink-type. Rheol Disperse Syst 1959:84–104.
[21] Dash, et al. Casson fluid flow in a pipe filled with a homogeneous porous medium. Int J Eng Sci 1996;34(10):1145–56.
[22] Khan A, et al. MHD flow of sodium alginate-based Casson type nanofluid passing through a porous medium with Newtonian heating. Scient Rep 2018;8(1):8645.
[23] Pham TV, Mitsoulis E. Entry and exit flows of Casson fluids. Canad J Chem Eng 1994;72(6):1080–4.
[24] Amanulla CH, et al. Computational analysis of non-Newtonian boundary layer flow of nanofluid past a semi-infinite vertical plate with partial slip. Nonlinear Eng 2018;7(1):29–43.
[25] Ghadikolaei SS, et al. Nonlinear thermal radiation effect on magneto Casson nanofluid flow with Joule heating effect over an inclined porous stretching sheet. Case Stud Therm Eng 2018;12:176–87.
[26] Das M, ey al.. Unsteady MHD chemically reactive double-diffusive Casson fluid past a flat plate in porous medium with heat and mass transfer. Heat Transf—Asian Res 2019;48(5):1761–77.
[27] Nadeem S, et al. MHD three-dimensional Casson fluid flow past a porous linearly stretching sheet. Alexandria Eng J 2013;52(4):577–82.
[28] Oyelakin IS, et al. Unsteady Casson nanofluid flow over a stretching sheet with thermal radiation, convective and slip boundary conditions. Alexandria Eng J 2016;55(2):1025–35.
[29] Ullah I, et al. Unsteady MHD mixed convection slip flow of Casson fluid over nonlinearly stretching sheet embedded in a porous medium with chemical reaction, thermal radiation, heat generation/absorption and convective boundary conditions. PLoS One1 2016;11(10):e0165348.

DOLAT KHAN received the M.S. degree in applied mathematics from the department of Mathematics City University of Science and Information Technology, Peshawar Pakistan. He received M.sc in Mathematics from the same university. He is the Ph.D. scholar of applied mathematics at King Mongkut's University of Technology Thonburi (KMUTT). He has published many research papers in different well-reputed high-impact factor international journals of the world. His most experience has been working in the academic sector. It has expertise in fluid dynamics, entropy generation, two-phase flows, MHD flows, nanofluids, fractional derivatives, integral transforms, exact solutions, and mathematical modeling. He has more than five years of academic and research experience in different reputed institutions in the city.

POOM KUMAM (Member, IEEE) received the B.Sc. degree in mathematics from Burapha University (BUU), the M.Sc. degree in mathematics from Chiang Mai University (CMU), and the Ph. D. degree in mathematics from Naresuan University (NU). He is currently a Full Professor with the Department of Mathematics, King Mongkut's University of Technology Thonburi (KMUTT). In 2008, he received a grant from Franco-Thai Cooperation for short-term research from the Laboratoire de Mathematiques, Universite de Bretagne Occidentale, France. He was also a Visiting Professor for a short-term research with Prof. A. T.-M. Lau with the University of Alberta, Edmonton, AB, Canada. His research interests include fixed point theory and applications, computational fixed-point algorithms, nonlinear optimization and control theory, and optimization algorithms. He has authored/coauthored over 796 research articles published in international peer reviewed journals. Moreover, he has delivered several talks in different international conferences all around the world.